



# Modelling effects of type of trees on urban air pollution with a computational fluid dynamics model

R. San Jose<sup>1</sup> · J. L. Perez-Camanyo<sup>1</sup>

Received: 26 May 2022 / Accepted: 15 August 2022 / Published online: 18 October 2022  
© The Author(s) 2022

## Abstract

Urban trees can change (increase and/or decrease) pollutant concentrations and this study assesses the effect of urban trees on main pollutant concentrations in a 1 km by 1 km area, in a high traffic density zone, in Madrid City (Spain) using numerical computational fluid dynamics (CFD) simulations. A real-life experiment was designed for 1 week of June 2017 with a spatial resolution of 5 m. A zone of vegetation in which the dominant species are broadleaf trees was included in the business as usual (BAU) simulation. The second scenario focused on changing the type of tree from broadleaf in the BAU scenario to needleleaf in the so-called ND scenario. The differences between ND simulation and BAU simulation provide information about the effects of the type of tree on the air quality (NO<sub>2</sub> and O<sub>3</sub>) of the area. The results of the simulations show a high sensitivity to changes in the type of tree in urban parks with strong impacts (hot spots) in several areas located several hundreds of meters away of the green park area. The results of these simulations will provide more knowledge on the effects of trees that will have to be taken into account when developing mitigation strategies for atmospheric pollution.

**Keywords** Urban air quality · CFD PALM4U · Trees

## Introduction

It has been demonstrated that exposure to air pollution has serious effects on citizens' health, e.g., it increases the number and severity of respiratory and cardiovascular diseases, which in turn leads to increased mortality (Pope 2000). Air quality is currently one of the most complex environmental challenges in large cities (Chekir and Ben Salem 2020). Transport, industrial activities, and energy demand (Zorpas et al. 2021) have increased in cities because of population growth, resulting in higher levels of air pollution for citizens to breathe with corresponding effects on their health (Banzhaf et al. 2014). Air pollution mainly affects those living in large urban areas (Mavrakakis et al. 2021), where transport emissions contribute most to the degradation of air quality (Kelishadi and Poursafa 2010). Urban air quality in streets

is controlled both by the meteorological and background air pollution characteristics of the atmosphere around the specific area, called (large-scale) boundary conditions, and by local-scale dynamic and chemical processes, mainly driven by turbulence. It is necessary to combine the advantages of three-dimensional (large-scale) Eulerian models, which can simulate meteorological conditions and urban background concentrations of all major air pollutants of interest, and (local urban-scale) street models, which can simulate air pollutant concentrations in complex urban canopy configurations. The complex spatial distribution of obstacles, which makes it difficult to ventilate pollution at some points, combined with high emissions from road traffic, generates pronounced concentration gradients of pollutants in cities. For cities, it is therefore essential to know the concentrations of pollutants with a high spatial resolution (1–10 m) in order to be able to identify the most severe pollution hotspots. In this sense, computational fluid dynamics (CFD) models are powerful tools that allow us to reproduce the dispersion of pollutants in the complex urban environments. Micro-scale models, such as CFD models, can be used to solve the turbulent flow equations at a higher spatial resolution (in the order of meters) to reproduce in detail the atmospheric processes in the urban canopy layer. These numerical tools

---

Responsible Editor: Antonis Zorpas.

---

✉ R. San Jose  
roberto@fi.upm.es

<sup>1</sup> Environmental Software and Modelling Group, Computer Science School, Technical University of Madrid (UPM), Madrid, Spain

support urban planners and other decision-makers by providing detailed knowledge about the effects of possible air pollution mitigation strategies. This evaluation of measures is done before their real implementation, which provides a priori knowledge of potential actions that may not achieve their pollution abatement targets (Caplin et al. 2019).

There are two main types of CFD models which are used for such simulations: (a) models based on the Reynolds-averaged Navier–Stokes (RANS) method, where the turbulence is fully parameterized, and therefore cannot provide information on the turbulence structures and their effects on atmospheric chemistry (Segura et al. 2021) and (b) large eddy simulation (LES) models that are able to resolve the turbulence (to some extent) and provide detailed information on the relevant flow variables (Maronga et al. 2015). Most previous urban CFD studies have employed the RANS method owing to its lower computational costs (Salim et al. 2011). Most LES-based pollutant dispersion studies investigated flow and ventilation characteristics in street canyons or other idealized structures (Han et al. 2018).

In this paper, we present the applicability of a LES model in a full three-dimensional (3D) real domain with multiple street canyons, open areas, trees, and buildings with different heights. In this experiment the CFD model is coupled to a mesoscale model; this allows the CFD model to use time-varying boundary conditions provided by mesoscale models. Several studies have demonstrated the good performance of using CFD models with boundary conditions given by mesoscale models to simulate dispersion in built-up areas (Miao et al. 2013). The state of the art in CFD atmospheric modelling is to couple CFD models with mesoscale models (Baklanov and Nuterman 2009). There are some examples of CFD simulations where initial and boundary conditions come from mesoscale models, such as Tewari et al. (2010) and Michioka et al. (2013) where reasonable calculated results were shown compared to observed data. CFD simulations improved significantly when results from mesoscale models were used as initial and boundary conditions (Nelson et al. 2016; Wyszogrodzki et al. 2012). For example, Kwak et al. (2015) improved the performance in simulating NO<sub>2</sub> and O<sub>3</sub> concentrations using the boundary conditions of the WRF-CMAQ (Community Multiscale Air quality) mesoscale system. A comprehensive review of air quality simulations by coupling CFD with mesoscale models can be found in Kadaverugu et al. (2019). These studies imply that coupling simulations between mesoscale models and CFD has the potential to become an effective tool for predicting local-scale plume dispersion under real meteorological conditions.

Despite significant effort, there is still a lack of research in non-idealized 3D environments, which restricts the ability to simulate pollutant concentrations at the street level in complex urban areas. In this study, we propose to run

a CFD–LES model with a chemical reaction model with meteorological and chemical boundary conditions from a mesoscale model to assess the pollutant dispersion in a realistic 3D city scenario. The decision to select a LES simulation instead of a RANS simulation is due to the fact that the LES has the potential to provide more accurate and reliable results than simulations based on the RANS approach. LES can resolve much of the relevant turbulence dynamics. Except for very simple flow situations, RANS models will produce less accurate results because they cannot reproduce a complete flow field. Although LES involves higher simulation complexity and much higher computational cost, for some time periods and specific areas (such as this experiment) there are computational resources available to run LES models. LES models are nowadays mainly used for scenario-specific simulation or process studies to obtain a deeper understanding of flow characteristics and their applications to air quality for example (Bergot et al. 2014). LES models are increasingly used for the study of airflow in model domains with realistic urban topography (Wurps et al. 2020) as in this study.

The growing computing power of high-performance computing and major advances in fluid dynamics have generated new research opportunities in air quality modelling in urban environments. In some works, simulation models of large eddies that resolve turbulence have already been applied to cities to investigate air pollution. In earlier research, other teams have successfully applied CFD models to simulate NO<sub>2</sub> variability in cities with high (meters) horizontal resolution. Usually for meteorology, several scenarios are considered, but without coupling a mesoscale model to provide initial and boundary conditions, that allow one to perform the CFD simulation with real meteorological data, as is done in this work. Most urban simulations with CFDs have considered a two-dimensional idealized street canyon or a simplified urban topology; however, in this case, a real complex urban area is modelled, using real trees, streets, and 3D buildings data. This work proposes a novel approach to combine complex mesoscale and microscale air quality models with traffic simulation tools that consider emissions data, regional and urban meteorology, and variety of chemical and physical mechanisms to simulate air pollution concentrations at different spatial scales.

Urban air pollution is also influenced by short- and long-range transport of gaseous and particulate pollutants from surrounding areas. This is also an important factor to take into account in modelling the air quality of a city, so tools to simulate the transport of pollutants out of cities will have to be included, as is done in this work, including a mesoscale model to provide boundary conditions for the microscale simulation. The dispersion of urban pollutants in the built environment is inherently a multi-scale problem, from the global to the urban scale. We propose to combine the advantages of 3D

Eulerian models, which can simulate urban background concentrations of the main air pollutants of interest, and the 3D urban model, which can simulate air pollutant concentrations in complex urban canopy configurations. If we apply a pollution dispersion model over an urban area, we must take into account what happens in and on the urban canopy to determine the spatial–temporal variation of the simulated air pollutants. The complexity from a computational point of view is how to solve the equations describing the behavior of the flows, which in these areas are turbulent and therefore unstable and heterogeneous. In this context, CFD models are powerful tools to reproduce the dispersion of pollutants taking into account the realistic characteristics of urban environments. Microscale models, such as CFD models, can be used to solve the turbulent flow equations at a higher spatial resolution (on the order of meters) to reproduce in detail the atmospheric processes in the urban canopy layer.

Urban vegetation is an important element influencing the dispersion of pollutants in the cities. In fact, the impacts of vegetation in urban areas and its application as a mitigation measure for urban air pollution is currently under discussion. This paper aims to provide additional scientific evidence to the urban air quality community on the impact of the type of tree on  $\text{NO}_2$  and  $\text{O}_3$  concentrations in a local area. Trees and urban vegetation in general influence air pollution through multiple processes: biogenic emissions, pollutant deposition, thermal-chemical processes, and turbulent dispersion. All these processes need to be included in air quality modelling simulations with high spatial resolution in urban areas. Several modelling techniques, especially through CFD, are being applied to study the impact of urban vegetation on pollutant dispersion (Abhijith et al. 2017). The impact of vegetation is a consequence of the aerodynamic effect, altering fluxes, and by the emission and deposition process, adding and removing pollutants to and from the air through their leaves. Several studies have found that the aerodynamic effect is greater than pollutant emitted or removal by deposition (Buccolieri et al. 2018). In some studies, the inclusion of vegetation has been shown to be beneficial by decreasing pollutant concentrations through deposition on trees, leaves, and other green infrastructure (Pugh et al. 2012). However, vegetation can also increase pollutant concentration in street canyons by obstructing wind circulation. In this study, we analyze and quantify the positive and/or negative impacts of trees in a downtown area of the city of Madrid (Spain) in a real 3D scenario including buildings and trees structures.

## Materials and methods

### Modelling tools

The CFD simulations were run using the parallelized large-eddy simulation model (PALM) adapted to urban areas

(PALM4U) for atmospheric flows (Maronga et al. 2019). PALM4U solves the 3D fields of wind and scalar variables (e.g., potential temperature and scalar concentrations). The performance of PALM over an urban-like surface has been validated against wind tunnel simulations as shown in previous LES and field studies (Park et al. 2015). Buildings are included as solid obstacles that react to the flow dynamics via form drag and friction forces. Natural and paved surfaces in urban environments are taken into account by using a multilayer soil model. It is well known that vegetation canopy effects on the surface–atmosphere exchange of momentum, energy, and mass can be rather complex and can significantly modify the structure of the atmospheric boundary layer (ABL), particularly in its lower part (Gery et al. 1989). It is thus not possible to describe such processes by means of the roughness length, surface fluxes of sensible heat, and latent heat as is done in mesoscale models because of the very high spatial resolution. In order to describe the complete 3D structure of individual trees, the plan canopy model uses canopy leave area density (LAD) and basal area density (BAD) as inputs. The plant canopy model is integrated within the detailed radiation model (which includes shadows). The direct, diffuse, and reflected short-wave and long-wave radiation is partially absorbed by individual grid boxes of plan canopy and transformed to sensible heat flux inside the vegetation. This heat flux is transferred into the atmosphere to increase of the air mass temperature. The plant canopy also emits the long-wave radiation according its current local temperature. The latent heat fluxes from the vegetation represent an important part of the heat balance in the urban canopy. In addition, a fully “online” coupled chemistry module is integrated into PALM4U. The chemical species are treated as Eulerian concentration fields that may react with each other, and possibly generate new compounds; in this experiment the chemistry mechanism CBM4 Carbon Bond Mechanism (Schrader et al. 2016) with 32 compounds and 81 reactions has been used. Gases are deposited using the DEPAC module (Grell et al. 2005).

Initial and lateral boundary chemical and meteorological conditions were derived from a simulation with the Weather Research and Forecasting and Chemistry model (WRF/Chem) (San José et al. 2015) with 1 km spatial resolution, so we are following an off-line nesting approach. Boundary conditions as updated every 1 h and data are interpolated linearly in time. Road traffic is the main source of air pollution in urban areas, with the primary emitted pollutants in gas phase being  $\text{NO}_x$  ( $\text{NO}$  and  $\text{NO}_2$ ),  $\text{CO}$ , and volatile organic compounds (VOC). We have combined the microscale traffic model Simulation of Urban Mobility (SUMO) with the EMIMO (San José et al. 2015) emission model, based on the detailed methodology (Tier 3) described in the EMEP/EEA Air Pollution Emission Inventory Guidebook, to provide the traffic emissions with high spatial and temporal resolution

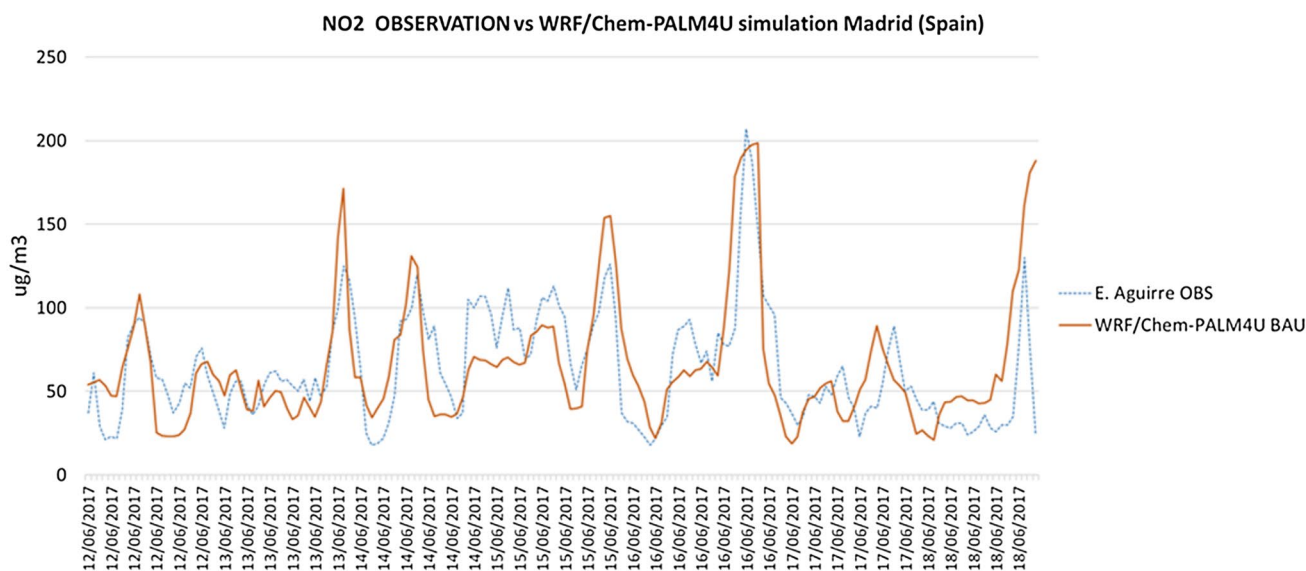


**Fig. 1** Time series of hourly concentrations of observed and WRF/Chem-PALM4U  $\text{NO}_2$  at the E. Aguirre station on June 12, 2017 to June 19, 2017

in the streets. The emission estimations are based on very detailed fleet composition data from the Madrid municipality and vehicle flow data from the SUMO model (Krajzewicz et al. 2012).

## Experiments

The PALM4U 3D computational domain was set up in Madrid (Spain). It is 1000 m by 1000 m by 300 m in height with a 3D spatial grid resolution of 5 m. GIS data about buildings, streets, and trees was obtained from the Madrid municipality open data service. The simulation area is selected to be an area with dimensions that allow it to be simulated with the available computational resources and that combines an area of trees and another area of buildings and streets with high traffic flow. It was also important to have at least one air quality station in the area in order to evaluate the performance of the simulation. In the area, there are two main roads with very high traffic flows and many street canyons. The area experiences high pollution  $\text{NO}_x$  episodes. In addition, there is an important green area (Retiro Park) in the model domain located at the southwest. The predominant species in the Retiro Park is the *Aesculus hippocastanum* known as the European horse chestnut with broad leaves. Trees represent 9.9% of the model area and buildings represent 43.9% of the model area. Water surface represents 1.4% of the model area. The simulation period was from June 12, 2017 to June 19, 2017, when high ozone levels were observed. The designed simulation requires 20,000 CPU hours per simulation (BAU, ND) and the simulation period was therefore limited to 1 week.

Two simulations were run. In the first one, the BAU (business as usual) simulation, is the reference simulation where the broadleaf trees are present. In this case, the vegetation type in the CFD model is set to “deciduous broadleaf trees” (number seven in the CFD model). In the second simulation, ND, the type of tree of the green area was changed to needleleaf. The differences (BAU–ND) show the impact of changing the type of trees from broadleaf to needleleaf in wind patterns and air pollution concentrations in all the area.

## Results and discussion

### Evaluation

In the reference area, one pollution monitoring station (E. Aguirre) is located near the Green Park. Figure 1 shows the evaluation of the WRF/Chem-PALM4U modelling tool against the monitoring station E. Aguirre with the hourly concentrations for  $\text{NO}_2$  (Fig. 1) and  $\text{O}_3$  (Fig. 2) on June 12, 2017 to June 19, 2017.

The following statistical parameters were calculated: normalized mean bias (NMB), root mean square error (RMSE) and Pearson’s temporal correlation ( $R^2$ ). In general terms,  $\text{NO}_2$  and  $\text{O}_3$  were slightly underestimated,  $\text{NO}_2$  by 7% and  $\text{O}_3$  by 24% based on the statistical indicator NMB. The squared hourly correlation coefficient ( $R^2$ ) is 0.6 for  $\text{NO}_2$  and 0.7 for  $\text{O}_3$ . The resulting RMSE is below  $30 \mu\text{g}/\text{m}^3$  for both pollutants. These values are in the standard range for this type of simulation in the scientific literature. The preliminary performance evaluation report indicates that the

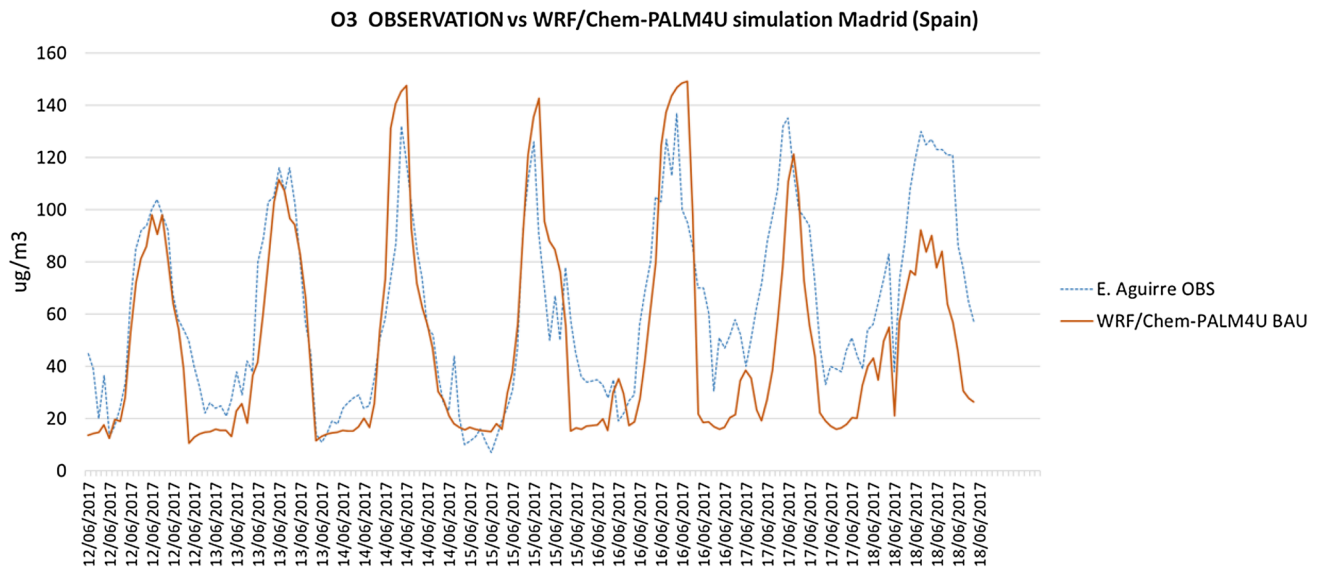


**Fig. 2** Time series of hourly concentrations of observed and WRF/Chem-PALM4U  $O_3$  at the E. Aguirre station on June 12, 2017 to June 19, 2017

BAU simulation for the  $NO_2$  and  $O_3$  dispersion with respect to the measured values in a specific location of the domain (within the  $5\text{ m} \times 5\text{ m}$  grid size in PALM4U) is appropriate. It is important to underline that the performance results of the CFD simulation are similar to the performance of the WRF/Chem simulation at  $1\text{ km}$  spatial resolution as the

surrounding concentrations have a strong influence on the local area concentrations.

### Impacts

Once the BAU simulation has been validated, the BAU and ND simulations were used to evaluate the effects of the type of tree on concentration levels of  $O_3$  (Fig. 3) and  $NO_2$  concentrations (Fig. 4). Figures 3 and 4 show the spatial distribution of changes (BAU–ND %) in  $O_3$  and  $NO_2$  concentrations when changing from broadleaf trees in the green zone to needleleaf trees. The trees change the distribution of  $O_3$  and  $NO_2$  concentrations, particularly at some hotspots. The effects of the type of tree are quite heterogeneous leading to decreases or increases of  $O_3$  and  $NO_2$  concentrations at pedestrian height.

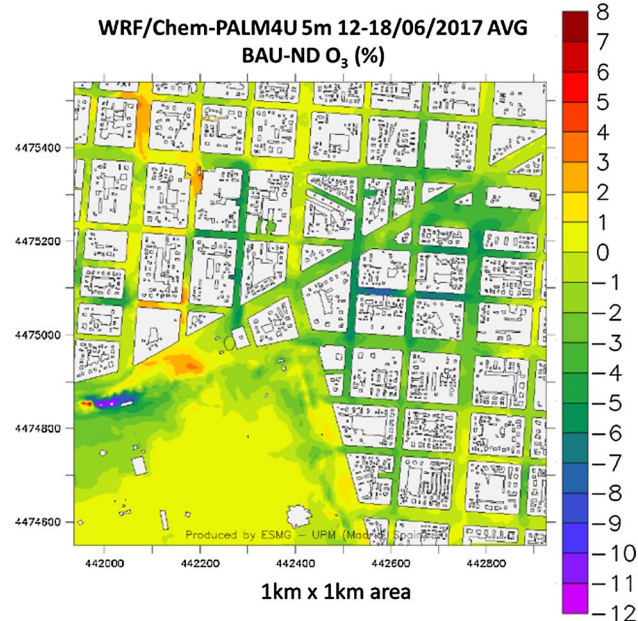


**Fig. 3** Spatial distribution with  $5\text{ m}$  spatial resolution of the effects of the type of tree (BAU–ND %) on  $O_3$  hourly averaged concentrations for the period June 12–18, 2017

Figure 3 shows the dispersive effect of the type of tree on  $O_3$  concentrations. The trees change the distribution of  $O_3$  concentrations, particularly at some hotspots. The effects of trees (Fig. 3) is quite heterogeneous leading to decreases or increases of  $O_3$  concentrations at pedestrian height. Needleleaf trees significantly increase  $O_3$  concentrations by up to 12% in the street closest to the green area (yellow areas) and decrease the concentrations by up to 8% at other points of the street. Figure 3 also suggests that trees change the pollutant concentrations in their surrounding streets and not only in the streets close to them. The  $O_3$  behavior was also influenced by the chemical reactions and controlled by the  $NO_x$ -limit and VOC-limit concentrations.

Changing the tree type from broadleaf to needleleaf involves changing the minimum canopy resistance parameter

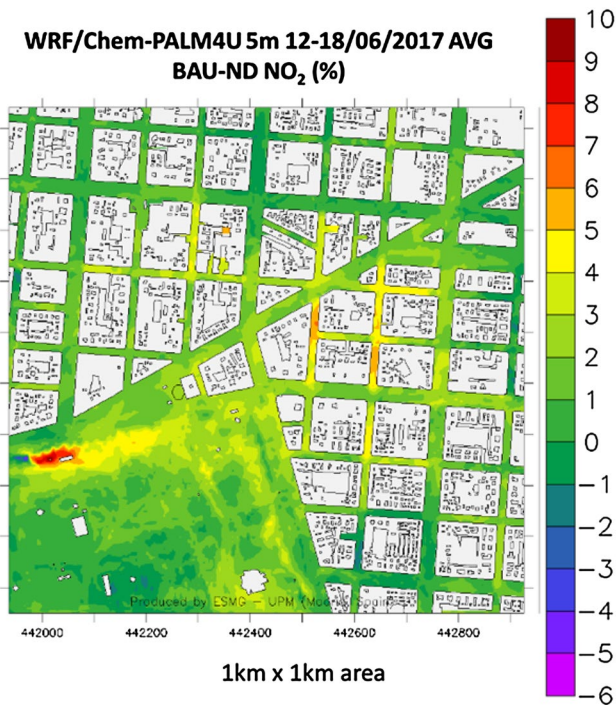


**Fig. 4** Spatial distribution with 5 m spatial resolution of the effects of the type of tree (BAU-ND %) on NO<sub>2</sub> hourly averaged concentrations for the period June 12–18, 2017

( $R_{c\_min}$ ) in Eq. 1.  $R_{c\_min}$  is 240 s/m for broadleaf trees (BAU) and 500 s/m for needleleaf trees (ND). This is the main parameter that changes from one simulation to another. Then in the ND simulation in the cells with trees, the canopy resistance ( $R_c$ ) is higher and therefore the latent heat flux ( $L$ ) is lower when calculated with Eq. 2 which causes an increase in temperature based on Eq. 3 for the energy balance. This calculation is included in the land surface model of the PALM4U model (Heus et al. 2010). This temperature increase causes O<sub>3</sub> concentrations to increase in 64.22% of the cells with an average increase of 1.93% and NO<sub>2</sub> concentrations to decrease in 90.67% of the grid cells with an average decrease of 1.69%.

$$R_c = \frac{R_{c\_min}}{LAI} f_1(R) f_2(Hm) f_3(e) \tag{1}$$

$$L = -\rho l_v \frac{1}{ra + rc} (q_v - q_{v,sat}) \tag{2}$$

$$C \frac{dT}{dt} = R_n - H - L - G \tag{3}$$

where  $R_c$  is the canopy resistance;  $R_{c\_min}$  is the minimum canopy resistance; LAI is the leaf area index;  $f_1$  is

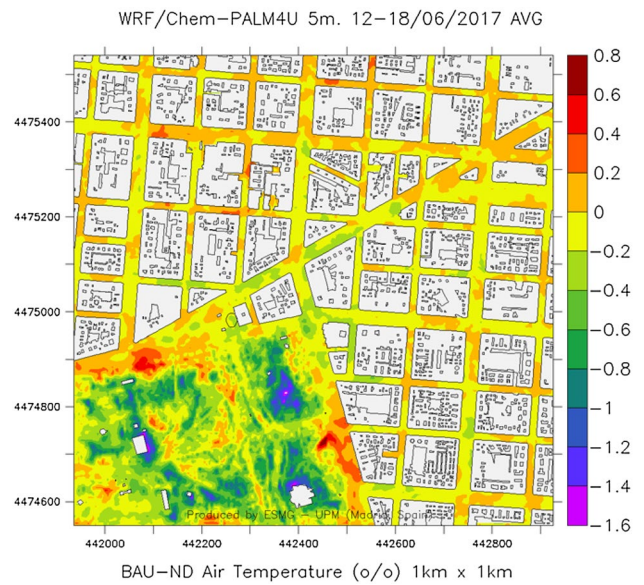


**Fig. 5** Spatial distribution with 5 m spatial resolution of the effects of the type of tree (BAU-ND %) on air temperature hourly averaged concentrations for the period 12–18 June, 2017

the correction factor based on solar radiation,  $R$  is the radiation,  $f_2$  is the correction factor based on soil humidity,  $Hm$  is the humidity;  $f_3$  is the correction factor based on water-vapor pressure deficit,  $e$  is the water-vapor pressure deficit;  $L$  is the latent heat flux;  $\rho$  is the air density;  $l_v$  is the latent heat of vaporization;  $ra$  is the aerodynamic resistance;  $rc$  is the canopy resistance for vegetation;  $q_v$  is the water vapor mixing ratio;  $q_{v,sat}$  is the water vapor mixing ratio at temperature  $T_0$ ;  $C$  is the heat capacity;  $T$  is the radiative temperature of the surface;  $R_n$  is the net radiation;  $H$  is the sensible heat flux;  $G$  is the ground (soil) heat flux.

Figure 5 shows the impact of the type of tree on the air temperature. The highest impacts occur in the green area where the trees are located; the needle-type trees increase the temperature (negative differences, green and blue colors) by up to 1.6%. Around the green area there are slight temperature increases which means that the temperature is somewhat higher with broadleaf trees. It is also important to note that the hypothetical change from broadleaf to needleleaf trees could produce temperature increases in some streets further away than 500–600 m from the green zone.

The first observation is that the impact of tree type on NO<sub>2</sub> concentration is different for each day. Needleleaf trees could increase NO<sub>2</sub> concentrations in the area for June 14 and 15, while a similar reduction in NO<sub>2</sub> concentrations would occur for June 13. The pollution reduction effect for June 18 is very important, as 90% of the domain (1 km<sup>2</sup>) would be reduced in NO<sub>2</sub> pollution if the trees in

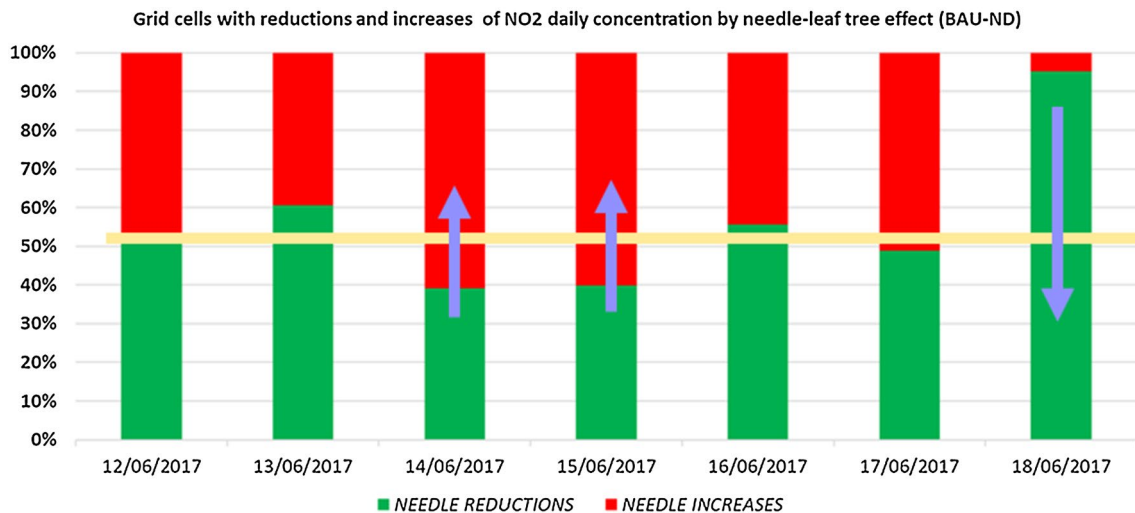


**Fig. 6** Percentage (%) of the domain with reductions (green) and increases (red) of NO<sub>2</sub> daily concentration by needle trees effects from June 12, 2017 to June 18, 2017

the park were of the needle type instead of the broadleaf type (Fig. 6).

## Conclusions

The CFD-LES-PALM4U 5 m spatial resolution model has been implemented over an area of 1 km × 1 km in downtown Madrid (Spain). The simulation reproduces pollutant concentration maps in the presence of boundary and top conditions supplied by the WRF/Chem 1 km simulation (nesting approach from the 5 km spatial resolution and 25 km spatial resolution covering all the Iberian Peninsula), real building morphology (3D), vegetation, and hourly emissions. The results obtained allow us to confirm that the modelling tool (WRF/Chem-PALM4U) successfully reproduces the concentration distributions of pollutants over urban areas. Analyses were performed to clarify the relative contributions of the type of tree to pollutant concentrations. To assess the impact of trees on concentrations, two simulations were run: the broadleaf trees simulation (BAU) and with needleleaf trees simulation (ND) in a green area of 1 km × 1 km area. In general, the spatial variability of concentrations with broadleaf and needleleaf trees within the study domain is notable with high impacts over the entire domain. The results show that the type of tree can increase or decrease the pollutant concentrations in a range of −12% to +10% in multiple areas of the full domain. We found that needleleaf trees can decrease NO<sub>2</sub> concentrations and increase O<sub>3</sub> concentrations. Trees in general and needleleaf trees reduce latent heat flux (Rc is greater than for broadleaf trees) and increase sensible, ground heat flux, and temperature, favoring O<sub>3</sub> formation.

The results are limited to a period of 1 week because of limited computational resources. Future work includes extending the simulation periods to 1 week per season to analyze the impact of trees under different temperatures and weather conditions.

Applying a high-resolution LES model over a real 3D urban topography can provide a large amount of detailed information about the flow and concentration fields. Our findings leave room for further studies, suggesting that the effects of urban vegetation on local air quality can be very complex, and have a substantial impact on local and potentially large urban areas. This work demonstrates how numerical simulation tools can generate information about potential mitigation actions that enable future urban planners to improve the air quality over urban areas (Bibri 2020; Ksibi et al. 2022).

**Acknowledgements** The UPM authors thankfully acknowledge the computer resources, technical expertise, and assistance provided by the Centro de Supercomputación y Visualización de Madrid (CES-VIMA). The authors thankfully acknowledge the computer resources at MareNostrum and the technical support provided by the Spanish Supercomputing Network (RES).

**Author contributions** All authors contributed to the study conception and design. Material preparation, data collection and analysis were performed by JLP-C. The first draft of the manuscript was written by RSJ and all authors commented on previous versions of the manuscript. All authors read and approved the final manuscript.

**Funding** Open Access funding provided thanks to the CRUE-CSIC agreement with Springer Nature. No funds, grants, or other support was received.

## Declarations

**Conflict of interest** On behalf of all authors, the corresponding author states that there is no conflict of interest.

**Open Access** This article is licensed under a Creative Commons Attribution 4.0 International License, which permits use, sharing, adaptation, distribution and reproduction in any medium or format, as long as you give appropriate credit to the original author(s) and the source, provide a link to the Creative Commons licence, and indicate if changes were made. The images or other third party material in this article are included in the article's Creative Commons licence, unless indicated otherwise in a credit line to the material. If material is not included in the article's Creative Commons licence and your intended use is not permitted by statutory regulation or exceeds the permitted use, you will need to obtain permission directly from the copyright holder. To view a copy of this licence, visit <http://creativecommons.org/licenses/by/4.0/>.

## References

- Abhijith K, Kumar P, Gallagher J, McNabola A, Baldauf R, Pilla F et al (2017) Air pollution abatement performances of green infrastructure in open road and built-up street canyon environments—a review. *Atmos Environ* 162:71–86. <https://doi.org/10.1016/j.atmosenv.2017.05.014>
- Baklanov A, Nuterman R (2009) Multi-scale atmospheric environment modelling for urban areas. *Adv Sci Res* 3(1):53–57. <https://doi.org/10.5194/asr-3-53-2009>
- Banzhaf E, de la Barrera F, Kindler A, Reyes-Paecke S, Schlink U, Welz J, Kabisch S (2014) A conceptual framework for integrated analysis of environmental quality and quality of life. *Ecol Ind* 45:664–668. <https://doi.org/10.1016/j.ecolind.2014.06.002>
- Bergot T, Escobar J, Masson V (2014) Effect of small-scale surface heterogeneities and buildings on radiation fog: large-eddy simulation study at Paris-Charles de Gaulle airport. *Q J R Meteorol Soc* 141(686):285–298. <https://doi.org/10.1002/qj.2358>
- Bibri S (2020) Data-driven environmental solutions for smart sustainable cities: strategies and pathways for energy efficiency and pollution reduction. *Euro-Mediterr J Environ Integr*. <https://doi.org/10.1007/s41207-020-00211-w>
- Buccolieri R, Santiago J, Rivas E, Sanchez B (2018) Review on urban tree modelling in CFD simulations: aerodynamic, deposition and thermal effects. *Urban Forestry Urban Greening* 31:212–220. <https://doi.org/10.1016/j.ufug.2018.03.003>
- Caplin A, Ghandehari M, Lim C, Glimcher P, Thurston G (2019) Advancing environmental exposure assessment science to benefit society. *Nat Commun*. <https://doi.org/10.1038/s41467-019-09155-4>
- Chekir N, Ben Salem Y (2020) What is the relationship between the coronavirus crisis and air pollution in Tunisia? *Euro-Mediterr J Environ Integr*. <https://doi.org/10.1007/s41207-020-00189-5>
- Gery M, Whitten G, Killus J, Dodge M (1989) A photochemical kinetics mechanism for urban and regional scale computer modeling. *J Geophys Res* 94(D10):12925. <https://doi.org/10.1029/jd094id10p12925>
- Grell G, Peckham S, Schmitz R, McKeen S, Frost G, Skamarock W, Eder B (2005) Fully coupled “online” chemistry within the WRF model. *Atmos Environ* 39(37):6957–6975. <https://doi.org/10.1016/j.atmosenv.2005.04.027>
- Han B, Baik J, Kwak K, Park S (2018) Large-eddy simulation of reactive pollutant exchange at the top of a street canyon. *Atmos Environ* 187:381–389. <https://doi.org/10.1016/j.atmosenv.2018.06.012>
- Heus T, van Heerwaarden C, Jonker H, Pier Siebesma A, Axelsen S, van den Dries K et al (2010) Formulation of the Dutch Atmospheric Large-Eddy Simulation (DALES) and overview of its applications. *Geosci Model Dev* 3(2):415–444. <https://doi.org/10.5194/gmd-3-415-2010>
- Kadaverugu R, Sharma A, Matli C, Biniwale R (2019) High resolution urban air quality modeling by coupling CFD and mesoscale models: a review. *Asia-Pac J Atmos Sci* 55(4):539–556. <https://doi.org/10.1007/s13143-019-00110-3>
- Kelishadi R, Poursafa P (2010) Air pollution and non-respiratory health hazards for children. *Arch Med Sci* 4:483–495. <https://doi.org/10.5114/aoms.2010.14458>
- Krajzewicz D, Erdmann J, Behrisch M, Bieker L (2012) Recent development and applications of SUMO—simulation of urban mobility. *Int J Adv Syst Meas* 5(3&4):128–138
- Ksibi M, Khadhraoui M, Kallel A, Aloulou F, Guargouri I, Daoud A et al (2022) Urban environmental issues in the metropolitan area of Sfax City, Tunisia: could an integrated management solve the problem? *Euro-Mediterr J Environ Integr* 7(1):29–48. <https://doi.org/10.1007/s41207-022-00295-6>
- Kwak K, Baik J, Ryu Y, Lee S (2015) Urban air quality simulation in a high-rise building area using a CFD model coupled with mesoscale meteorological and chemistry-transport models. *Atmos Environ* 100:167–177. <https://doi.org/10.1016/j.atmosenv.2014.10.059>
- Maronga B, Gryschka M, Heinze R, Hoffmann F, Kanani-Sühring F, Keck M et al (2015) The Parallelized Large-Eddy Simulation Model (PALM) version 4.0 for atmospheric and oceanic flows: model formulation, recent developments, and future perspectives. *Geosci Model Dev* 8(8):2515–2551. <https://doi.org/10.5194/gmd-8-2515-2015>
- Maronga B, Gross G, Raasch S, Banzhaf S, Forkel R, Heldens W et al (2019) Development of a new urban climate model based on the model PALM—project overview, planned work, and first achievements. *Meteorol Z* 28(2):105–119. <https://doi.org/10.1127/metz/2019/0909>
- Mavrikis A, Kapsali A, Tsiros I, Pantavou K (2021) Air quality and meteorological patterns of an early spring heatwave event in an industrialized area of Attica, Greece. *Euro-Mediterr J Environ Integr*. <https://doi.org/10.1007/s41207-020-00237-0>
- Miao Y, Liu S, Chen B, Zhang B, Wang S, Li S (2013) Simulating urban flow and dispersion in Beijing by coupling a CFD model with the WRF model. *Adv Atmos Sci* 30(6):1663–1678. <https://doi.org/10.1007/s00376-013-2234-9>
- Michioka T, Sato A, Sada K (2013) Large-eddy simulation coupled to mesoscale meteorological model for gas dispersion in an urban district. *Atmos Environ* 75:153–162. <https://doi.org/10.1016/j.atmosenv.2013.04.017>
- Nelson M, Brown M, Halverson S, Bieringer P, Annunzio A, Bieberbach G, Meech S (2016) A case study of the weather research and forecasting model applied to the joint urban 2003 tracer field experiment. Part 2: gas tracer dispersion. *Bound-Layer Meteorol* 161(3):461–490. <https://doi.org/10.1007/s10546-016-0188-z>
- Park S, Baik J, Lee S (2015) Impacts of mesoscale wind on turbulent flow and ventilation in a densely built-up urban area. *J Appl Meteorol Climatol* 54(4):811–824. <https://doi.org/10.1175/jamc-d-14-0044.1>
- Pope C (2000) Epidemiology of fine particulate air pollution and human health: biologic mechanisms and who's at risk? *Environ Health Perspect* 108:713. <https://doi.org/10.2307/3454408>
- Pugh T, MacKenzie A, Whyatt J, Hewitt C (2012) Effectiveness of green infrastructure for improvement of air quality in urban street canyons. *Environ Sci Technol* 46(14):7692–7699. <https://doi.org/10.1021/es300826w>
- Salim S, Cheah S, Chan A (2011) Numerical simulation of dispersion in urban street canyons with avenue-like tree plantings:



- comparison between RANS and LES. *Build Environ* 46(9):1735–1746. <https://doi.org/10.1016/j.buildenv.2011.01.032>
- San José R, Pérez J, Balzarini A, Baró R, Curci G, Forkel R et al (2015) Sensitivity of feedback effects in CBMZ/MOSAIC chemical mechanism. *Atmos Environ* 115:646–656. <https://doi.org/10.1016/j.atmosenv.2015.04.030>
- Schrader F, Brümmer C, Flechard C, Wichink Kruit R, van Zanten M, Zöll U et al (2016) Non-stomatal exchange in ammonia dry deposition models: comparison of two state-of-the-art approaches. *Atmos Chem Phys* 16(21):13417–13430. <https://doi.org/10.5194/acp-16-13417-2016>
- Segura R, Badia A, Ventura S, Gilabert J, Martilli A, Villalba G (2021) Sensitivity study of PBL schemes and soil initialization using the WRF-BEP-BEM model over a Mediterranean coastal city. *Urban Clim* 39:100982. <https://doi.org/10.1016/j.uclim.2021.100982>
- Tewari M, Kusaka H, Chen F, Coirier W, Kim S, Wyszogrodzki A, Warner T (2010) Impact of coupling a microscale computational fluid dynamics model with a mesoscale model on urban scale contaminant transport and dispersion. *Atmos Res* 96(4):656–664. <https://doi.org/10.1016/j.atmosres.2010.01.006>
- Wurps H, Steinfeld G, Heinz S (2020) Grid-resolution requirements for large-eddy simulations of the atmospheric boundary layer. *Bound-Layer Meteorol* 175(2):179–201. <https://doi.org/10.1007/s10546-020-00504-1>
- Wyszogrodzki A, Miao S, Chen F (2012) Evaluation of the coupling between mesoscale-WRF and LES-EULAG models for simulating fine-scale urban dispersion. *Atmos Res* 118:324–345. <https://doi.org/10.1016/j.atmosres.2012.07.023>
- Zorpas A, Navarro-Pedreño J, Jeguirim M, Dimitriou G, Almendro Candel M, Argirusis C et al (2021) Crisis in leadership vs waste management. *Euro-Mediterr J Environ Integr*. <https://doi.org/10.1007/s41207-021-00284-1>